Korean J. Chem. Eng., 33(3), 986-996 (2016)
DOI: 10.1007/s11814-015-0212-x

pISSN: 0256-1115
eISSN: 1975-7220

Analysis of thermophysical property data of HI_x components for I_2 crystallizer design in sulfur-iodine process to produce hydrogen

Byung Heung Park*, Kyoung-Soo Kang, and Jeong Won Kang***,†**

*Department of Chemical and Biological Engineering, Korea National University of Transportation, 50, Daehak-ro, Chungju-si, Chungbuk 27469, Korea
**Hydrogen Energy Research Center, Korea Institute of Energy Research, 152, Gajeong-ro, Yuseong-gu, Daejeon 34129, Korea
***Department of Chemical and Biological Engineering, Korea University, 145, Anam-ro, Seongbuk-gu, Seoul 02841, Korea
(*Received 16 March 2015 • accepted 11 October 2015*)

Abstract—I_2 crystallization could be a technical option in HI decomposition section of SI thermochemical water splitting process to increase process efficiency. Design of a crystallizer requires experimental data as well as corresponding equations for thermophysical properties of HI_x solution, which is a named ternary solution of H_2O, HI, and I_2. However, so far, there are no available analyses on them. We collected experimental data and corresponding equations with temperature parameters and compared the equations with the data to analyze their accuracy and credibility. Thermal conductivity was updated in this work while keeping a structure of a corresponding equation. Relative deviations were estimated for liquid density, thermal conductivity, viscosity, and heat capacity and summarized with temperature for H_2O, HI, and I_2. Solution density and viscosity of binary H_2O-HI solution were also analyzed with an empirical equation under a limited condition and with predictable methods exhibiting satisfactory consistency.

Keywords: SI Process, Hydrogen Production, Thermophysical Properties, Iodine, Hydrogen Iodide

INTRODUCTION

The uses and applications of hydrogen have been gradually expanded and the focus on its role has been changed from a chemical agent in various industries to an energy carrier. Hydrogen is considered as an ideal replacement for fossil fuels toward zero-emission of carbon dioxide future especially in a transportation sector. Hydrogen production from water using heat and/or electricity from nuclear energy could practically attain the goal of zero carbon dioxide emission throughout an entire process, including feedstock, energy in use, and final waste.

In Korea, nuclear energy has been supplied to meet the increasing domestic energy demand and contributed in stabilizing the consumer price of electricity. The experience obtained by the development, construction, and operation of nuclear reactors and the awareness on the prospect of the hydrogen economy have motivated the government to set up a roadmap for the nuclear hydrogen production. In 2004, the Nuclear Hydrogen Development and Demonstration (NHDD) project was launched to realize nuclear-based hydrogen production technology by 2021 [1]. A reference nuclear hydrogen system consists of a VHTR (Very high temperature reactor) system for heating helium, a sulfur-iodine (SI) water splitting process for producing hydrogen, and a heat exchange loop that transports the heat from the reactor to the SI process. The first-phase studies of NHDD (2004 to 2005) have already presented candidate plant designs based on a 200 MWth (megawatt thermal) VHTR core and SI thermochemical process [2]. At the second-phase studies (2006 to 2009), the VHTR and the SI process were improved and validated to a level that can be applied to the basic design of the NHDD system. The next phase studies (to 2016) are in progress to develop core technologies.

The direct thermal decomposition of water is possible at very high temperature (over 2,000 °C). However, thermochemical water

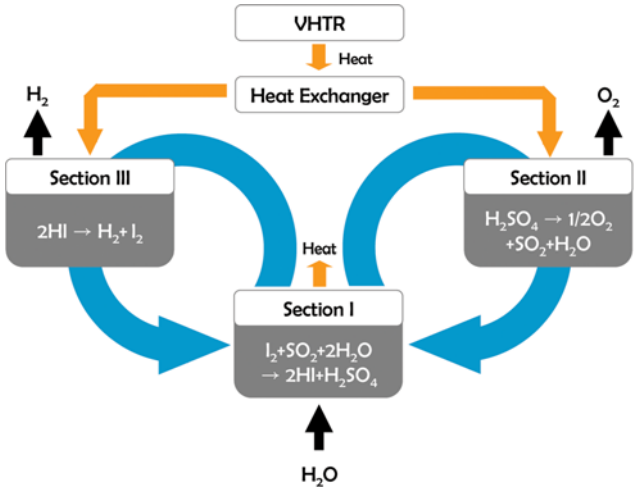

Fig. 1. Schematic description of SI thermochemical process coupled to VHTR.

†To whom correspondence should be addressed.
E-mail: jwkang@korea.ac.kr

splitting cycles can decompose water into hydrogen and oxygen at a lower temperature than its direct decomposition condition through a series of chemical reactions associated with some recyclable chemical agents. The SI process described in Fig. 1 is one of the most advanced thermochemical water splitting cycles [3], enabling mass production of hydrogen without emitting carbon dioxide when coupled to nuclear heat energy. The highest temperature (close to 1,000 °C) required in SI process is well matched with the outlet temperature of a coolant circulating a high-temperature gas-cooled reactor at around 950 °C. Therefore, the heat from the reactor can be directly used to produce hydrogen. In NHDD program, it has been conceptualized that a 200 MWth VHTR would supply heat to five modules of the SI water splitting processes [4]. Korea Institute of Energy Research (KIER) has led experimental researches and demonstration of the SI process according to NHDD program [5,6], especially focusing on HI decomposition and H_2 production.

The SI process proposed by General Atomics (GA) [7] has been actively studied by several research groups [8-13], including in Korea, Japan, and China. The SI cycle is composed of three sections: the Bunsen section (Section I), the H_2SO_4 separation and decomposition section (Section II), and the HI_x section (Section III). HI_x is a named mixture of HI, I_2, and H_2O. Some flowsheet simulation studies have integrated these sections and estimated the thermal efficiency of the whole cycle over 40% [14], which was defined as the higher heating value of hydrogen (285.8 kJ/mol-H_2) over net energy demand. Among the sections, Section III is the most significant one in determining the overall efficiency.

HI_x exhibits an azeotropic behavior which limits the HI concentration lower than azeotropic one in a conventional distillation column, since the same composition of vapor with liquid is evaporated when a solution reaches the azeotropic point. Therefore, to effectively separate HI from HI_x and avoid vaporization of excess H_2O for higher efficiency, advanced distillation processes such as an extractive distillation [15] and a reactive distillation [16] have been adopted. In addition, electro-electrodialysis (EED) technology [17] was applied to concentrate HI before the distillation and the introduction of I_2 removal step prior to the EED step was considered to decrease the burden on EED [18]. Low solubility of I_2 in the solution enables the removal to be by a crystallization technique. Therefore, the first step of Section III to separate HI from HI_x associates with I_2 crystallization, EED, and HI distillation as shown in Fig. 2.

The results of efficiency estimation would be nonsense if inappropriate thermophysics and thermodynamic methods and data are used. In this work, we collected and reviewed accessible web-based and published data as well as available correlation equations for the design of process equipment in Section III, including the I_2 crystallizer, the EED cell, the HI distillation column, and the HI decomposer. The process utilizes heat transfer through the HI_x solution and forced or gravitational sedimentation of solid I_2 particles on a crystallizer. As a consequence, the reactor size and the operation time of the process depend on the solution properties such as density, heat conductivity, viscosity, and heat capacity. Therefore, before designing a reactor, it is important to investigate the solution property and examine applicable equations. In this study, the credibility of the correlation equations was also assessed using the collected data, and some coefficients for thermophysical property equations were regressed and presented when an equation could not properly describe the corresponding data. The investigated thermophysical properties would be also very useful in developing such processes.

THERMOPHYSICAL PROPERTIES OF PURE H_2O, HI, AND I_2

1. Basic Properties

The molecular weight, critical properties, and characteristic temperatures such as the normal boiling point and the melting point are basic thermophysical properties of a chemical compound; they are generally required in various correlation equations both for pure substances and mixtures to describe volumetric, transport, and/or calorimetric properties. They are easily found in many databases and handbooks. In this study, the values were collected from some widely referred data books [19-22] in the chemical engineering field and compared in Table 1. The table contains molecular weight (M_w), the normal melting point (T_m), the normal boiling point (T_b), and the critical properties of temperature (T_c), pressure (P_c), and molar volume (V_c) with acentric factor (ω) for each substances. No remarkable differences between the figures are found except for the critical pressure and volume of HI. The critical pressure and volume are frequently used as important input constants when a correlation equation is used to estimate a temperature and/or composition depending property of mixtures; thus it is necessary to compare the effect of the difference on other properties.

In practice, an equation of state (EoS) is applicable to present relations among pressure, volume, and temperature of components in a gaseous phase. Cubic EoSs have been successfully applied to the HI_x system [23-27], which requires critical properties to determine equation parameters. For example, the well-known Peng-Robinson (PR) cubic EoS expresses the relation of volume (V), pressure (P), and temperature (T) as follows with gas constant (R= 8.314×10^{-5} bar·m^3/mol·K) and three parameters of a, b, and dimen-

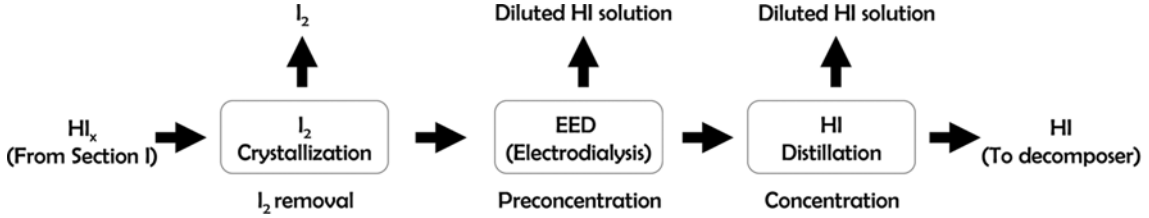

Fig. 2. Flow diagram of section III.

Table 1. Thermophysical constants of H_2O, HI, and I_2

	M_w	T_m [K]	T_b [K]	T_c [K]	P_c [bar]	V_c [cm^3/mol]	ω
H_2O	18.015	273.15	373.15	647.13[a] 647.14[b,c]	220.55[a] 220.64[b] 220.6[c]	55.95[a,b] 56[c]	0.3449[a] 0.344[b]
HI	127.912	222.38[a,b] 222.39[c] 222.35[d]	237.55[a] 237.57[b] 237.6[c] 237.85[d]	423.85[a] 423.90[b] 424.0[c]	83.10[a] 90.00[b] 83.1[c]	121.9[a] 132.70[b]	0.0381[a] 0.038[b]
I_2	253.809	386.75[a] 386.76[b] 386.85[c] 386.65[d]	457.56[a,b] 457.55[c] 457.5[d]	819.15[a] 819.00[b,c]	116.54[a]	155.00[a,b,c]	0.1115[a]

[a]Yaws [19]
[b]Poling et al. [20]
[c]Lide [21]
[d]Green and Perry [22]

sionless α calculated from critical properties (temperature T_c and pressure P_c) and three dimensionless parameters of acentric factor (ω), κ parameter, and reduced temperature (T_r) (Eqs. (1) to (6)),

$$P = \frac{RT}{V-b} - \frac{a\alpha}{V^2+2bV-b^2} \quad (1)$$

$$a = \frac{0.457235R^2T_c^2}{P_c} \quad (2)$$

$$b = \frac{0.077796RT_c}{P_c} \quad (3)$$

$$\alpha = \{1+\kappa(1-T_r^{0.5})\}^2 \quad (4)$$

$$\kappa = 0.37464 + 1.54226\omega - 0.26992\omega^2 \quad (5)$$

$$T_r = T/T_c \quad (6)$$

As for HI, the critical property from the reference [19] {T_c [K], P_c [bar], w}={423.85, 83.10, 0.0381} and the critical property from the reference [20] {423.90, 90.00, 0.038} produce different sets of PR EoS parameters as {a [Pa×m^6/mol^2], b [m^3/mol]}={0.6833, 3.299×10^{-5}} and {0.6310, 3.046×10^{-5}}, respectively. From 573 to 723 K, where HI decomposes in Section III, we investigated the effect of the difference on PVT behavior of HI and found that the molar volumes of gaseous HI described by PR EoS with the two different parameter sets give almost identical behaviors and negligible differences as shown in Fig. 3. At 40 bar where HI decomposed

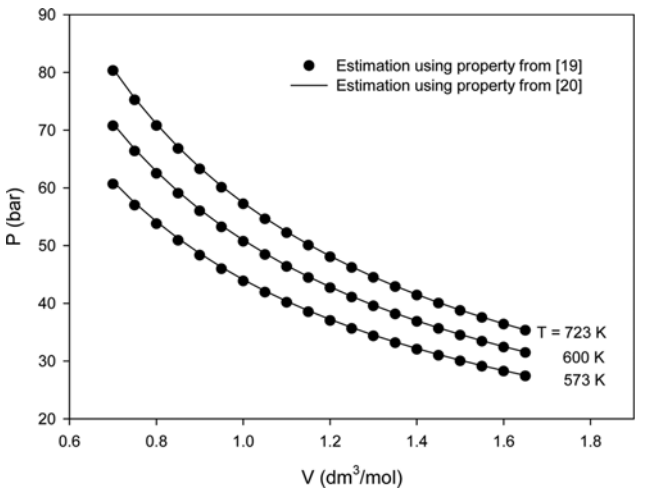

Fig. 3. Comparison of pure HI vapor PVT behavior calculated by PR EoS with two different sets of parameters estimated from different critical properties listed in Table 1.

Table 2. Density of H_2O, HI, and I_2

	Liquid (coefficients of Eq. (7) or (8))								Solid		
	A_d	B_d	C_d	D_d	T_{min} [K]	T_{max} [K]	Eq.	Ref.	ρ [g/cm^3]	T [K]	Ref.
H_2O	0.32500 5.459 4.9669	0.27000 0.30542 0.27788	647.13 647.13 647.13	0.23000 0.081 0.18740	290.00 273.16 333.15	647.13 333.15 403.15	(7) (8) (8)	[19] [28] [28]	0.9168	273.15	[19]
HI	1.04638	0.28826	423.85	0.28571	222.38	423.85	(7)	[19]	3.5370	78.0	[19]
I_2	1.63746	0.33313	819.15	0.33550	386.75	737.24	(7)	[19]	4.8203 4.933 4.93	386.75 293.15 293.15	[19] [21] [22]

into H_2 and I_2, the second set estimates only 0.61% greater molar volumes than those from the first set at 600 K. However, cautious consideration should be taken when selecting a set of thermophysical constants of HI for accounting for mixture properties by various correlation equations associated with critical properties.

2. Liquid and Solid Density

If solid I_2 particles sink through HI_x solution by gravitational or external force, the density difference would be a critical factor for separation time. Therefore, we have searched for density data and correlation equations as an important property. Yaws [19] has proposed the following Eq. (7) to express the temperature dependence of liquid density, in the unit of g/cm^3, of pure substances with the coefficients given in Table 2. As for H_2O, we found Eq. (8) was also usable with different temperature coefficients with respect to temperature ranges [28] as given in Table 2. In addition, we collected the available solid density data and listed in the same table. Note that some of the maximum temperatures in Table 2 were much higher than boiling points at standard pressure and close to the critical temperatures. Therefore, it is assumed that the equations can be used at elevated pressure. The assumption is valid because the liquid density is not sensitive to pressure.

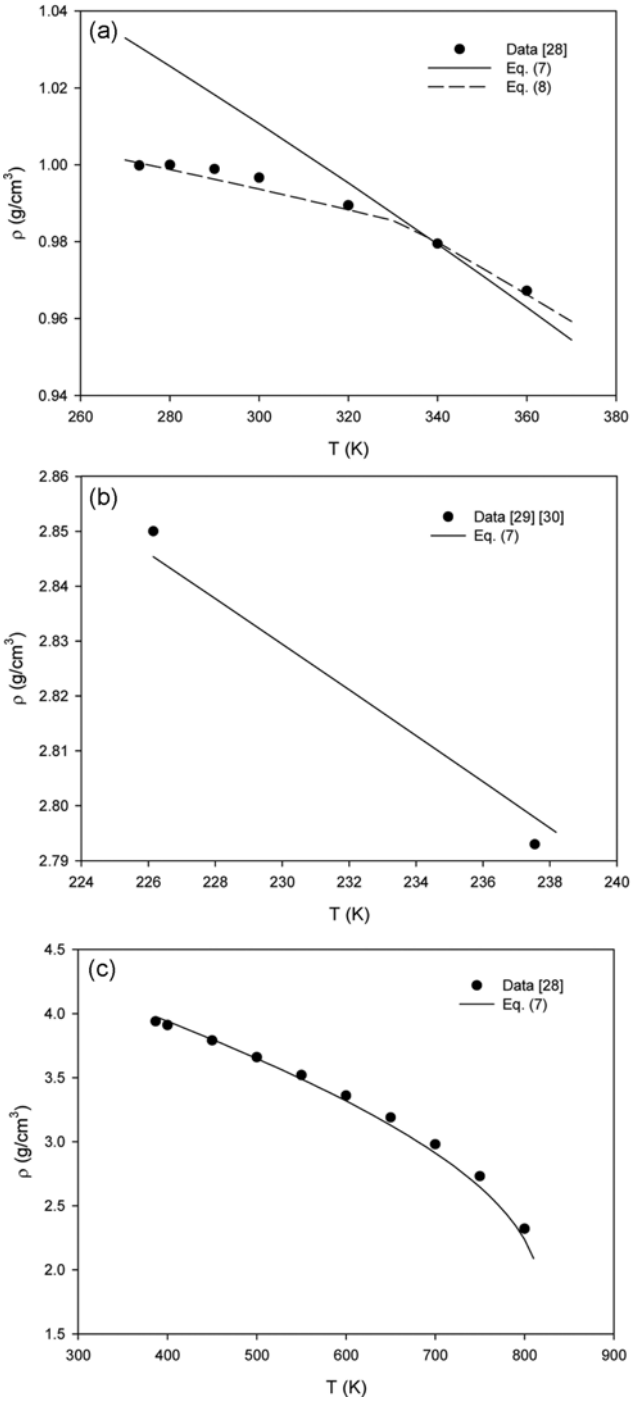

Fig. 4. Comparison of data and calculated liquid densities by correlation equations: (a) H_2O, (b) HI, and (c) I_2.

$$\rho[\mathrm{g/cm^3}] = A_d \times B_d^{-(1-T[K]/C_d)^{D_d}} \tag{7}$$

$$\rho[\mathrm{kmol/m^3}] = (A_d / B_d^{\{1+(1-T[K]/C_d)^{D_d}\}}) \tag{8}$$

The correlation equations were compared with experimental liquid density data [28-30] in Fig. 4. In the figure, the temperature range of I_2 was extended beyond the maximum temperature limit given in Table 2 to examine the equation at high temperature where experimental data were available. As for H_2O, Eq. (8) gives better results than Eq. (7). The liquid densities of HI are known only at two different temperatures. We excluded the data of liquid density 2.85 g/cm^3 at 268.45 K [31] because the temperature is much higher than the HI normal boiling point and could collect just two points as presented in Fig. 4(b). However, the temperature range of Eq. (7) for HI includes 268.45 K and the density was comparatively calculated to 2.66 g/cm^3 at the temperature. Eq. (7) with the temperature coefficients given in Table 2 well describes the change of I_2 liquid density as shown in Fig. 4(c) even beyond the given temperature range. However, the equation underestimates the density as temperature increases and the deviations from experimental data increased.

3. Liquid Thermal Conductivity

For crystallization by cooling, usually a heat sink embraces a reactor. Therefore, the time required for bulk solution to reach an operation temperature depends on thermal conductivity of the solution. If the thermal conductivity is too low, the heat transfer area should be increased and a reactor design should reflect the feature. A temperature-dependent correlation equation and its parameters for liquid thermal conductivity for pure substances were found in a web-based databank [32]. The databank offers a polynomial equation as follows and temperature parameters are listed in Table 3. Some of the maximum temperatures in Table 3 were much higher than the normal boiling points and close to the critical temperatures. It is assumed that the data can be applied to the case of high pressure. The assumption is valid because liquid thermal conductivity is not pressure dependent.

$$k[\mathrm{W/m\cdot K}] = A_k + B_k \times T[K] + C_k \times T[K]^2 \tag{9}$$

By using Eq. (9) and Table 3, the liquid thermal conductivities were plotted with temperature and the results compared with reported data [28] in Fig. 5. The given equation and the coefficients for H_2O successfully regenerated the reported data. However, the coefficients for HI and I_2 were not acceptable for the data repro-

Table 3. Temperature coefficients for thermal conductivity Eq. (9)

	A_k	B_k	C_k	T_{min} [K]	T_{max} [K]	Ref.
H_2O	−0.3838	5.254E-3	−6.369E-6	273	623	[32]
HI	0.2599	−4.3E-5	−9.098E-7	223	383	[32]
	−3.9873E-3	4.389E-4	−9.4E-7	273.15	423.15	This work
I_2	0.134	4.296E-5	−2.031E-7	386	785	[32]
	5.5342E-2	−2.175E-4	2.27E-7	386.8	785	This work
I_2 (s)	1.0492	−2.8901E-3	2.966E-6	250	386.8	This work

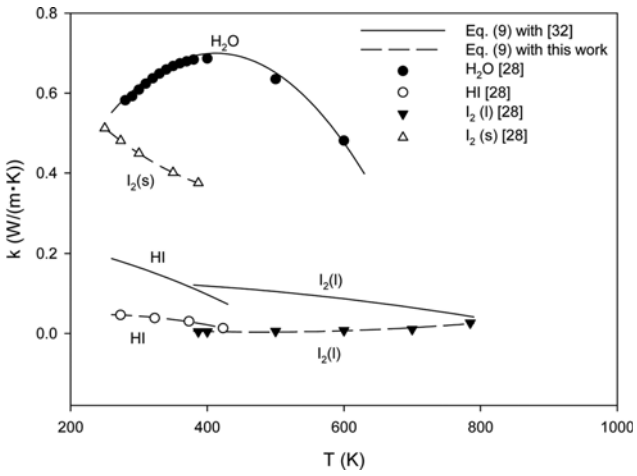

Fig. 5. Comparison of data and calculated thermal conductivity by Eq. (9).

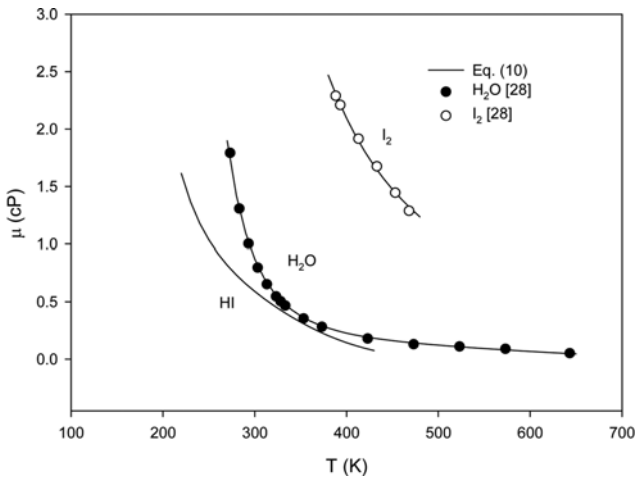

Fig. 6. Comparison of data and calculated liquid viscosity by Eq. (10).

duction as recognized in Fig. 5. Therefore, the temperature coefficients had to be re-determined based on the experimental data for Eq. (9). We carried out a regression of experimental data for new coefficients by least square method. The absolute averaged deviations from the experimental data were reduced from 9.98×10^{-2} to 8.59×10^{-4} W/m·K and from 7.98×10^{-2} to 1.70×10^{-3} W/m·K for HI and I_2, respectively, when newly regressed coefficients were used. The coefficients obtained in this work are also given in Table 3 with the collected ones and the liquid thermal conductivity behaviors with temperature described by the updated coefficients are co-plotted in Fig. 5. In this study, the thermal conductivity of solid I_2 was regressed as well and the coefficients were also presented in Table 3. Note that new experimental data is required to confirm the coefficients.

4. Liquid Viscosity

When a particle sinks in a fluid, drag force occurs opposite to its direction. The drag force cannot be estimated without the viscosity of the fluid. Therefore, we also found viscosity data and equations for the HI_x system. KDB [32] provides a correlation equation and temperature coefficients for liquid viscosity. The viscosity (μ) is expressed as the following equation in the unit of cP depending on temperature in K.

$$k[W/m\cdot K]=A_k+B_k\times T[K]+C_k\times T[K]^2 \quad (10)$$

Given temperature coefficients as Table 4, the behaviors of liquid viscosities were drawn with temperature and compared with reported data [28] in Fig. 6. The equation could depict the behaviors with good agreements with data of H_2O and I_2. However, there are no available data to be compared with for HI liquid viscosity. The maximum temperatures in Table 4 are much higher than the normal boiling points. Therefore, it is assumed that Eq. (10) can be used with Table 4 at high pressures since the liquid viscosity was not significantly affected by pressure.

5. Liquid Heat Capacity

Liquid heat capacity is an important property for the crystallizer design because this property determines waste heat amount. The liquid heat capacity (C_p in J/mol×K) equations are found in web-based database [32,33]. KDB [32] provides a temperature depen-

Table 4. Temperature coefficients for liquid viscosity

	A_v	B_v	C_v	D_v	T_{min} [K]	T_{max} [K]	Ref.
H_2O	−24.71	4209	0.04527	−3.376E-5	273.15	643.15	[32]
HI	−21.58	2337	0.07336	−9.717E-5	223.15	423.15	[32]
I_2	−2.083	1195	−4.566E-4	1.08E-7	387.15	473.15	[32]

Table 5. Temperature coefficients for liquid heat capacity

	A_c	B_c	C_c	D_c	E_c	T_{min} [K]	T_{max} [K]	Ref.
H_2O	50.8107	0.21294	−6.30969E-4	6.4831E-7	-	273.15	623.15	[32]
	−203.606	1523.290	−3196.413	2474.455	3.85533	298	500	[33]
HI	−343.482	4.1418	−1.42092E-2	1.65640E-5	-	223.15	413.15	[32]
I_2	80.6692	6.8556E-8	−8.72435E-8	3.72313E-8	4.7358E-10	386.75	457.67	[33]

dent equation with four coefficients while NIST [33] offers an extended equation with five coefficients using scaled-down temperature of t.

$$C_p[J/mol\cdot K]=A_c+B_c\times T[K]+C_c\times T[K]^2+D_c\times T[k]^3 \quad (11)$$

$$C_p[J/mol\cdot K]=A_c+B_c\times t+C_c\times t^2+D_c\times t^3+E_c/t^2 \quad (12)$$

where, t=T[K]/1000

The temperature coefficients for the both Eqs. (11) and (12) are collected as Table 5. It is emphasized that the maximum temperatures in Table 5 were also much higher than the normal boiling points as other properties. It is assumed that the equation can be used for high pressure. The assumption is valid because liquid heat capacity does not depend much on pressure.

The experimental data of liquid heat capacity for I_2 was not obtainable. The data of the other substances [21,34] were compared with the correlation equations in Fig. 7. As for H_2O, Eq. (12) presented better results than Eq. (11) because Eq. (12) uses one more temperature coefficient than Eq. (11). We collected only three points for liquid HI heat capacity [34]. The data showed a decreasing behavior with temperature, but Eq. (12) gave the opposite behavior as well as large deviations from the data. Eq. (12) is not adequate to estimate heat capacity of liquid HI.

THERMOPHYSICAL PROPERTIES OF BINARY H_2O-HI SOLUTION

There are not so many thermophysical property data of binary or ternary solutions of HI, I_2, and H_2O. As for ternary mixtures, Kubo et al. [35] reported on the data of density and viscosity focusing on Bunsen reaction (Section I) products, that is, HI_x solution with or without minute H_2SO_4. They measured density and viscosity up to 90 and 40 °C, respectively. However, they did not show numeric experimental data and, thus, the authors could not use the data to determine the applicability of correlation equations. We could only obtain the density and viscosity of binary H_2O-HI solution data with respect to temperature as numeric experimental values in some references [36,37].

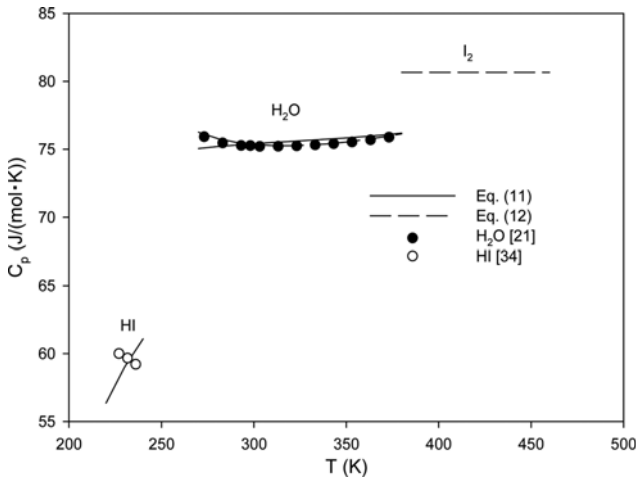

Fig. 7. Comparison of data and calculated liquid heat capacity by Eqs. (11) and (12).

1. Density of Binary H_2O-HI Solution

HI is highly soluble in H_2O to 234 g/100 g H_2O at 10 °C. Hydriodic acid forms when HI is dissolved in H_2O, which exhibits an azeotrope at 56.9 wt% HI at 127 °C with density of 1.709 g/cm^3 [34] and the concentration ranges of the density data were limited to about 57 wt%. A correlation equation between HI concentration (c, wt%) and density for the solution at 25 °C up to 45 wt% was shown as follows [28].

$$\rho[g/cm^3]=-1.33539\times10^{-8}C^4+1.72047\times10^{-6}C^3 +2.25058\times10^{-5}C^2+7.2801\times10^{-3}C+0.99676 \quad (13)$$

Kubo et al. [35] proposed an equation correlating their experimental data with the compositions and temperature as Eq. (14). Though the equation is for HI_x solution density, it can be used for H_2O-HI solution by applying x_{I2}=0.

$$\rho[g/cm^3]=\sum_{j=0}^{2}\sum_{i=0}^{2}c_{ij}T^i x_{latom}^j \quad (14)$$

$$x_{latom}^j=\frac{x_{HI}+2x_{I_2}}{x_{HI}+2x_{I_2}+x_{H_2O}} \quad (15)$$

where, T (K), x'_{latom}, and x are temperature, mole fraction of I atom defined by Eq. (15), and mole fraction, respectively. The coefficients (c_{ij}) in Eq. (14) were regressed by a least square method as summarized in Table 6.

Eq. (13) seems to an empirical correlation and its applicability is very limited because the temperature was fixed at 25 °C. The appli-

Table 6. Coefficients of Eq. (14) for liquid density of HI_x [35]

c_{ij}		j		
		0	1	2
i	0	3.505E-01	1.570E+01	−1.174E+01
	1	4.572E-03	−6.255E-02	5.929E-02
	2	−8.010E-06	9.052E-05	−9.098E-05

cation of Eq. (14) is also limited within the experimental conditions where the coefficients (c_{ij}) were regressed. Therefore, we tried to find general relation equations and examined them by comparing with the experimental data. Poling et al. [20] collected a number of various property estimation methods. As for densities of liquid solutions, three methods are adoptable: Chueh-Prausnitz method, Li method, and HBT method. They are general approaches associated with mixing rules, including critical properties of solution components. Details of the equations are in the reference [20] and, in this work, we presented the results obtained by using the equations. Note that the first set of critical properties for HI [19] given in Table 1 was used in the three correlation methods.

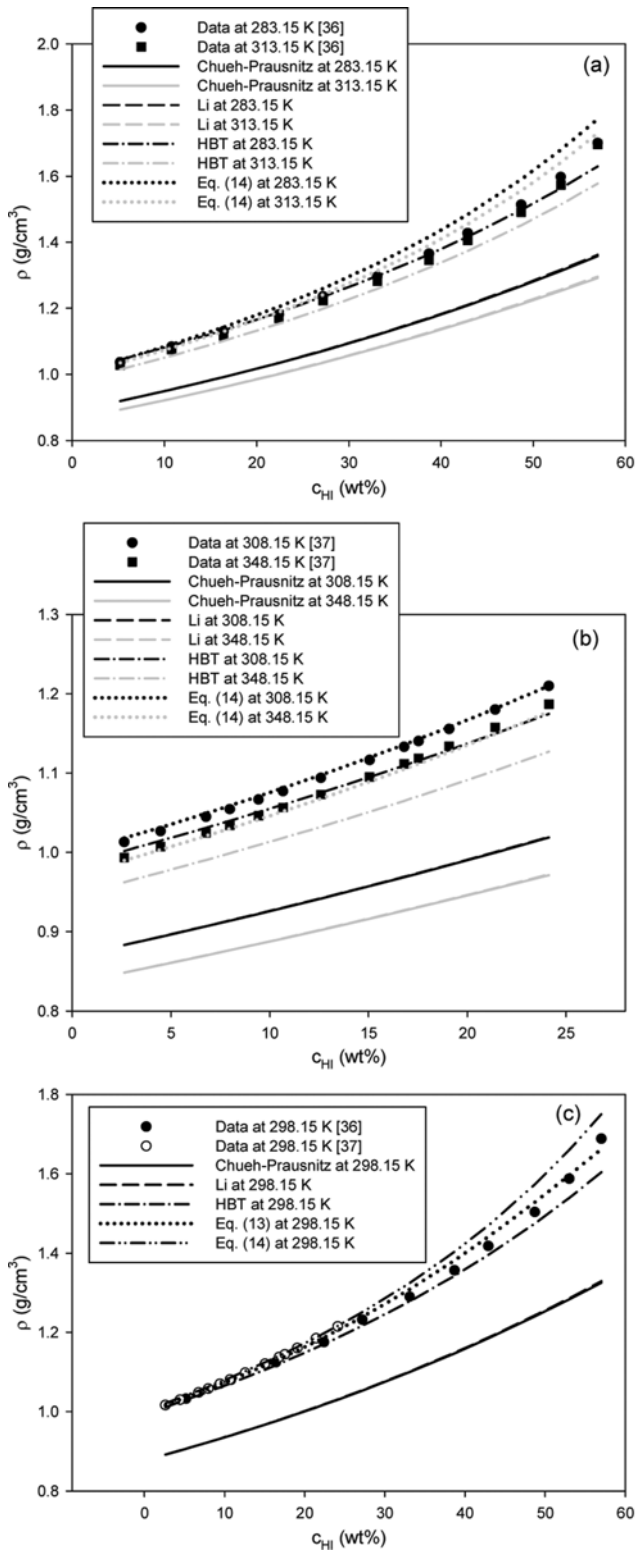

Fig. 8. Dependence of HI-H_2O solution density on HI concentration.

Fig. 8 shows that the correlation methods well followed the behavior of the data. The data of Nishikata et al. [36] covered 283.15 to 313.15 K up to 57 wt%. In Fig. 8(a) the selected data at 283.15 and 313.15 K are presented with the four correlation methods, including Eq. (14). The binary H_2O-HI solution density from 298.15 to 348.15 K was measured by Herrington et al. [37] and the data at 308.15 and 348.15 K were plotted with the results of the correlation methods in Fig. 8(b) as a selected illustration. In Fig. 8(c) the experimental data are compared with each other at 298.15 K, and the result from Eq. (13) is also shown with the four correlation methods. In general, the estimated results from the correlation equations monotonically increased with concentration. Chueh-Prausnitz and Li methods estimated nearly identical behavior and superimposed. Chueh-Prausnitz and Li methods underestimated the binary density and the HBT method showed the least deviation among the three general methods. Though the application of Eq. (14) was reduced to binary solution system, it accurately followed experimental behavior at relatively low- and mid-concentration range as presented in Fig. 8(b). However, when the concentration of HI exceeded about 25 wt%, Eq. (14) showed an overestimating tendency as found in Fig. 8(a) and (c). At 298.15 K, Eq (13) well agreed with the experimental data (see Fig. 8(c)). As for the binary H_2O-HI density, it could be concluded that Eq. (13) would be recommended to use at 298.15 K, while Eq. (14) would be preferred to the other three general methods at the other temperatures.

2. Viscosity of Binary H_2O-HI Solution

Nishikata et al. [36] measured the viscosity of aqueous hydriodic acid from 283.15 to 313.15 K with HI composition up to 57 wt%. Minimum points on 33.0, 28.7, and 16.4 wt% at 283.15, 288.15, and 293.15 K, respectively, were found, while the viscosity of aqueous HCl solution increased monotonically. In practice, the parabolic behavior of the viscosity is difficult to describe without fitting parameter(s). Poling et al. [20] proposed three correlation equations for liquid mixture viscosity: Grunberg and Nissan, UNIFAC-VISCO, and Teja and Rice method. Furthermore, they added a comment that neither Grunber and Nissan nor the UNIFAC-VISCO method is recommended for aqueous solution. Therefore, we applied the Teja and Rice method, which required an interaction parameter (y_{12}) as a temperature-dependent fitting parameter. Details of the method can be found in reference [20].

An empirical equation describing the liquid viscosity of HI_x solution was found in a reference [35]. The equation related the viscosity with temperature and compositions by a reduced form of Eq. (10) associated with two coefficients reflecting composition dependence as follows:

$$\ln\mu[\mathrm{cP}]=A+B/T[\mathrm{K}] \tag{16}$$

$$A=d_0+d_1x_{HI}+d_2x_{I_2} \tag{17}$$

Table 7. Coefficients of Eqs. (17) and (18) for liquid viscosity of HI_x [35]

	i		
	0	1	2
d_i	−6.800	16.77	−5.173
e_i	2001	−4332	3306

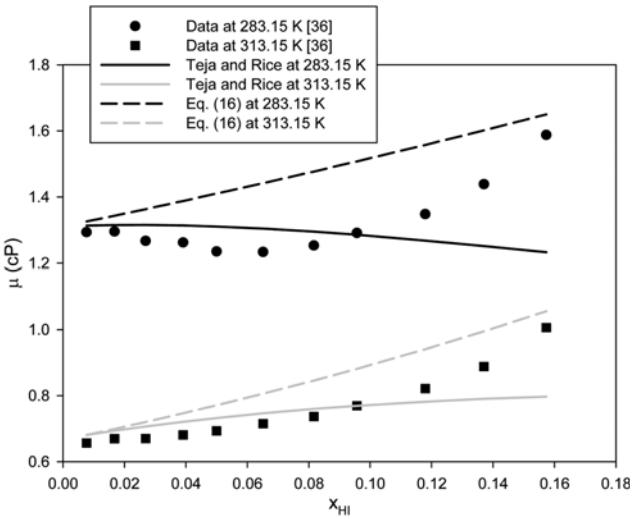

Fig. 9. Dependence of HI-H_2O solution viscosity on HI composition.

$$B=e_0+e_1x_{HI}+e_2x_{I_2} \quad (18)$$

The coefficients (d and e) on the mole fractions (x) in Eqs. (17) and (18) were determined by least square method and presented by Kubo et al. [35] as Table 7. For the viscosity of a binary HI-H_2O system, Eq. (16) can be used by setting $x_{I_2}=0$ in Eqs. (17) and (18).

As an illustration, the estimated values were compared with the experimental data at 283.15 and 313.15 K in Fig. 9 with respect to the mole fraction of HI (x_{HI}). The interaction parameters for Teja and Rice method were determined to minimize the deviations from the experimental data: ψ_{12}=1.12 and 1.20 at 283.15 and 313.15 K, respectively. The behavior estimated by Teja and Rice method did not correctly describe the experimental values. As the composition increased, the deviations became intensified since the method estimated oppositely decreasing viscosity with composition. Therefore, the direct use of Teja and Rice method was not favored for the binary solution. Solution viscosity calculated by Eq. (16) was co-plotted in Fig. 9. Eq. (16) estimated monotonically increasing viscosity with respect to the HI composition and the deviations from the experimental data were decreased at the both ends of the composition range ($0<x_{HI}<0.16$).

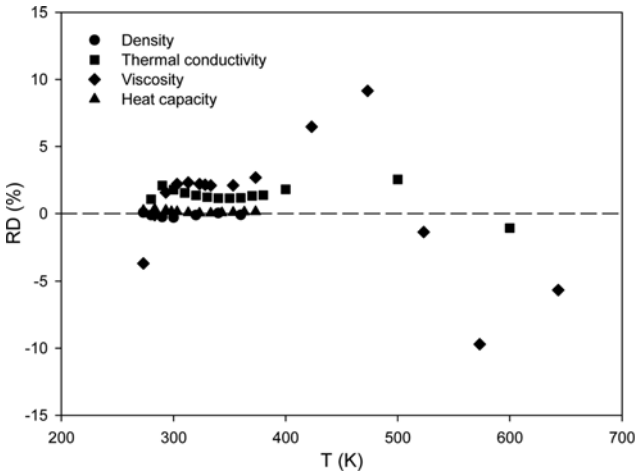

Fig. 10. Relative deviations by correlation equations for H_2O.

ACCURACY OF CORRELATION EQUATIONS

1. Pure Properties

We collected various equations describing dependence of thermophysical properties on temperature of pure elements. The accuracy of the equations should be examined for further application in process modeling and simulation. Relative deviations (RDs) defined by Eq. (19) were adopted to evaluate the accuracy for each property.

$$RD(\%)=100\times\frac{M^{cal}-M^{data}}{M^{data}} \quad (19)$$

H_2O is one of the most well-known substances and its properties are already enough. For liquid density, thermal conductivity, viscosity, and heat capacity, correlation equations accurately reproduce experimental data. As for liquid density and heat capacity, Eqs. (8) and (12) were used to estimate RDs unlike the other substances, respectively. An RD diagram with temperature for H_2O revealed that RDs are less than 3% except for the viscosity (Fig. 10). When temperature is lower than 400 K, where H_2O is liquid under atmospheric pressure, RDs were less than 3% for viscosity. An averaged absolute RD (AARD) for each property was estimated and presented in Table 8.

Table 8. Summary on the accuracy of the correlation equations for pure components

	Density		Thermal conductivity		Viscosity		Heat capacity	
	No. of data	AARD (%)	No. of data	AARD (%)	No. of data	AARD (%)	No. of data	AARD (%)
H_2O	7	0.1438	14	1.475	15	3.566	12	0.1361
HI	2	0.1684	4	2.955	-	-	3	1.749
I_2	10	1.520	6	20.73	6	1.055	-	-

$AARD(\%)=\frac{100}{n}\sum_i\frac{|M_i^{cal}-M_i^{data}|}{M_i^{data}}$, where n is the number of data

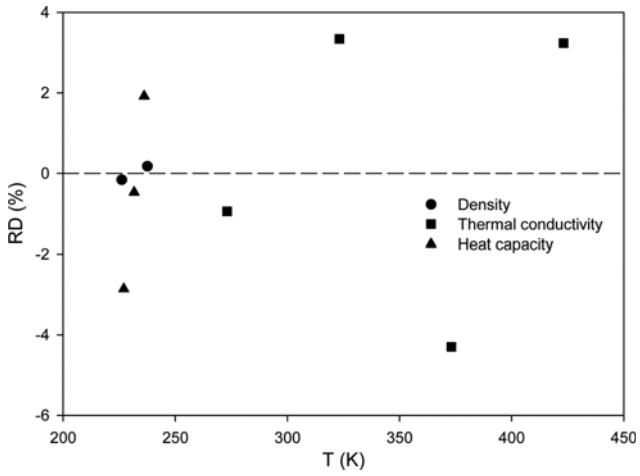

Fig. 11. Relative deviations by correlation equations for HI.

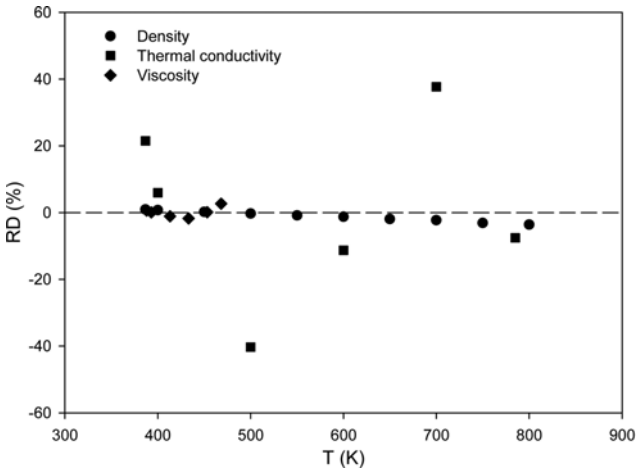

Fig. 12. Relative deviations by correlation equations for I_2.

For HI, experimental data on three properties of density, thermal conductivity, and heat capacity were compared with the correlation equations and new temperature coefficients determined in this work were used to estimate RDs on thermal conductivity. In general, there were not many data for liquid HI. In particular, only 2 liquid density data are available. RDs determined by using the available data showed that the correlation equations could reproduce the data within 4% as shown in Fig. 11. However, in case of liquid heat capacity, Eq. (11) with the given temperature coefficients was not adequate to describe the decreasing tendency with temperature as presented in Fig. 7 even though RDs were relatively satisfactory within the narrow temperature range of experimental data. AARD for HI is also summarized in Table 8. At present, the values of the AARD are not enough due to their small number of data. However, if more data is available, the AARD would be more meaningful. Measurement of the data is desired.

We could not obtain liquid heat capacity data of I_2. Therefore, RDs on three properties of density, thermal conductivity, and viscosity were plotted with temperature in Fig. 12 and AARD is listed in Table 8. The temperature coefficients regressed in this study were used for liquid thermal conductivity. As for density and viscosity, it was revealed that the equations could be used with credibility within the temperature ranges. However, the thermal conductivity results were not satisfactory even though the new temperature coefficients were regressed in this work. The thermal conductivity of liquid I_2 is very low; for example, at 600 K, thermal conductivity of liquid I_2 is 7.4×10^{-3} W/m·K while that of H_2O is 0.6864 W/m·K. Therefore, small deviations from the experimental data were emphasized when calculated by relative values. In addition, the quadratic polynomial equation of Eq. (9) was inadequate to describe the monotonically increasing behavior of liquid I_2 thermal conductivity with temperature.

2. HI-H_2O Solution Properties

As for binary HI-H_2O solution properties, the accuracies of the correlation equations were evaluated using Eq. (19). The number of data and AARD (%) are summarized in Table 9. Eq. (14) presents the most accurate results for density by 1.442 % of AARD. Note that the coefficients of Eq. (14) were regressed from the ternary experimental data [35] even though a reduced form for a binary solution was applied. However, no fitting parameters were required on HBT method, which showed compatible results with those of Eq. (14). Therefore, HBT may be more reliable when predicting the solution density out of the experimental data range used for determining the coefficients of Eq. (14). The viscosity behavior of HI-H_2O solution is complicated, exhibiting concave up change within the range of $5.2<c_{HI}$ (wt%)<57 (or $0.008<x_{HI}<0.157$). It seems that the equations of Teja and Rice method as well as Eq. (16) proposed by Kubo et al. [35] could not properly describe the viscosity changes with the composition as presented in Fig. 9 and Table 9.

Table 9. Summary on the accuracy of the correlation equations for liquid HI-H_2O solution

Density					Viscosity		
No. of data*	AARD (%)				No. of data#	AARD (%)	
	Chueh-Prausnitz	Li	HBT	Eq. (14)		Teja and Rice	Eq. (16)
155	15.18	15.12	2.091	1.442	76	6.497	11.103

$$\mathrm{AARD}(\%)=\frac{100}{n}\sum_i\frac{\left|M_i^{cal}-M_i^{data}\right|}{M_i^{data}}$$, where n is the number of data

*$283.15<T\ (K)<348.15$ and $2.63<c_{HI}$ (wt%)<57

#$283.15<T\ (K)<313.15$ and $5.2<c_{HI}$ (wt%)<57

CONCLUDING REMARKS

Introduction of an I_2 crystallizer into a process stream in Section III of the well-known SI thermochemical process for massive hydrogen production could be a plausible option for increasing whole process efficiency. The removal of I_2 prior to EED could reduce the burden on the following processes such as EED and distillation.

As for the I_2 crystallizer to remove I_2 from the HI_x solution, density, thermal conductivity, viscosity, and heat capacity are the most important properties since the equipment utilizes heat transfer through a solution and I_2 particles are recovered after sedimentation caused by gravitational and/or external force. We investigated thermophysical properties on HI_x components. We collected experimental data and corresponding empirical correlation equations from published as well as web-based references and, then, examined the equations to report their deviations from the data.

First, the pure properties of its components were investigated. The critical properties of HI were inconsistent, but the difference was not critical for PVT behavior calculated by PR EoS. However, the values should be cautiously chosen for other properties because many correlation equations use critical properties as input constants. As for pure liquid density, two equations were collected with temperature parameters for H_2O. The second type equation (Eq. (8)) should be used for H_2O while the first type (Eq. (7)) is applicable to the others and AARDs were estimated as 0.1438, 0.1684, and 1.5196 for H_2O, HI, and I_2, respectively. For liquid thermal conductivity, the coefficients from one reference [30] did not reproduce data of liquid HI and I_2. New coefficients were regressed by using experimental data in this work. With the updated coefficient, AARDs were 1.4749, 2.9548, and 20.732 for H_2O, HI, and I_2, respectively. Still, in case of I_2, the deviations were relatively large due to the very low values of I_2 thermal conductivity. Liquid viscosity data of H_2O and I_2 were also compared with a corresponding equation and, as a result, 3.5656 and 1.0547% AARDs were calculated for H_2O and I_2, respectively. A correlation equation for heat capacity gave satisfactory accuracy for H_2O and HI. However, it could not describe the monotonic decreasing behavior with temperature for HI.

There were scarce data for mixture properties. We found only density and viscosity of binary H_2O-HI solution. In practice, the mixture properties were correlated by predictable methods. Therefore, we compared three widely applicable methods and two empirical equations (Eqs. (13) and (14)) with experimental data for mixture density; Chueh-Prausnitz, Li, and HBT methods for predictable methods. Among them, HBT method and the empirical equations reproduced the experimental data satisfactorily. For the viscosity of binary H_2O-HI solution, the Teja and Rice method and an empirical equation were tried to use for describing experimental data. However, both methods were not suitable to follow the viscosity behavior with composition.

We examined the correlation equations for liquid density, thermal conductivity, liquid viscosity, and heat capacity and found that the accuracy of the equations was relatively low for H_2O viscosity and I_2 thermal conductivity. The properties of mixtures are usually correlated by equations which require pure component properties from experimental data or by correlation equations. In this respect, the properties of HI_x solution should be estimated from equations for mixtures using correlation equations for pure compounds since the experimental data of pure compounds might not be available for the required HI_x properties. Though the density of HI-H_2O solution can be estimated, the applicable temperature is limited below 343.15 K and the viscosity of the HI-H_2O solution cannot be estimated with accuracy. Experimental data and estimation equations for the properties of HI_x solution are very few. The results would be useful when coupled to a process design software for an I_2 crystallizer and other equipment, and we also expect that the information could be further used for the other purposes such as property model development.

ACKNOWLEDGEMENT

This study was performed under the mid- and long-term Nuclear R&D Projects supported by the Ministry of Science, ICT and Future Planning (2012M2A8A2025688), Republic of Korea.

ABBREVIATIONS

AARD : averaged absolute relative deviation
EED : electro-electrodialysis
EoS : equation of state
GA : general atomics
KDB : Korea Thermophysical Properties Data Bank
KIER : Korea Institute of Energy Research
NHDD : nuclear hydrogen development and demonstration
PR : Peng-Robinson
RD : relative deviation
SI : sulfur-iodine
VHTR : very-high-temperature reactor

REFERENCES

1. Y.-J. Shin, J.-H. Kim, J. Chang, W.-S. Park and J. Park, *Nuclear hydrogen production project in Korea. In: Nuclear production of hydrogen*, Third Information Exchange Meeting Oarai, Japan 5-7 October 2005, NEA (2006).
2. J.-H. Chang, Y.-W. Kim, K.-Y. Lee, Y.-W. Lee, W. J. Lee, J.-M. Noh, M.-H. Kim, H.-S. Lim, Y.-J. Shin, K.-K. Bae and K.-D. Jung, *Nucl. Eng. Technol.*, **39**, 111 (2007).
3. A. Basile and A. Iulianelli Ed., *Advances in hydrogen production, storage and distribution*, Woodhead Publishing (2014).
4. IAEA, *Proc. Non-electrical applications of nuclear power: Seawater desalination, hydrogen production and other industrial applications*, IAEA-CN-152 (2009).
5. K.-S. Kang, C.-H. Kim, W.-C. Cho, S.-U. Jeong, C.-S. Park and K.-K. Bae, *Nucl. Eng. Des.*, **256**, 67 (2013).
6. T. D. B. Nguyen, Y.-K. Gho, W. C. Cho, K. S. Kang, S. U. Jeong, C. H. Kim, C.-S. Park and K.-K. Bae, *Appl. Energy*, **115**, 531 (2014).
7. J. L. Russell Jr., K. H. McCorkle, J. H. Norman, J. T. Porter II, T. S. Roemer, J. R. Schuster and R. S. Sharp, *Proc. 1st WHEC*, Miami Beach, Fl., 1-3 March (1976).
8. L. C. Brown, G. E. Besenbruch, R. D. Lentsch, K. R. Schultz, J. F.

Funk, P. S. Pickard, A. C. Marshall and S. K. Showalter. *High efficiency generation of hydrogen fuels using nuclear power*, GA-A24285 (2003).
9. A. Le Duigou, J.-M. Borgard, B. Larousse, D. Doizi, R. Allen, B. C. Ewan, G. H. Priestman, R. Elder, R. Devonshire, V. Ramos, G. Cerri, C. Salvini, A. Giovannelli, G. De Maria, C. Corgnale, S. Brutti, M. Roeb, A. Noglik, P.-M. Rietbrock, S. Mohr, L. de Oliveira, N. Monnerie, M. Schmitz, C. Sattler, A. O. Martinez, D. de L. Manzano, J. C. Rojas and S. Dechelotte, *Int. J. Hydrogen Energy*, **32**, 1516 (2007).
10. K. Seiji, K. Shinji, H. Ryutaro, O. Kaoru, N. Mikihiro and N. Shinpichi, *Int. J. Hydrogen Energy*, **32**, 489 (2007).
11. F. Gelbard, J. C. Andazola, G. E. Naranjo, C. E. Velasquez and A. R. Reay, *High pressure sulfuric acid decomposition experiments for the sulfur-iodine thermochemical cycle*, SAND2005-5598 (2005).
12. W.-C. Cho, C.-S. Park, K.-S. Kang, C.-H. Kim and K.-K. Bae, *Nucl. Eng. Des.*, **239**, 501 (2009).
13. P. Zhang, C. Z. Chen, L. J. Wang and J. M. Xu, *Int. J. Hydrogen Energy*, **35**, 2883 (2010).
14. S. Kasahara, S. Kubo, R. Hino, K. Onuki, M. Nomura and S. Nakao, *Int. J. Hydrogen Energy*, **32**, 489 (2007).
15. J. H. Norman, G. E. Besenbruch, L. C. Brown, D. R. O'Keefe and C. L. Allen, *Thermochemical water-splitting cycle, bench-scale investigations, and process engineering*, DOE/ET/26225-1 (1982).
16. S. Goldstein, J. M. Borgard and X. Vitart, *Int. J. Hydrogen Energy*, **30**, 619 (2005).
17. S. Kasahara, S. Kubo, K. Onuki and M. Nomura, *Int. J. Hydrogen Energy*, **29**, 579 (2004).
18. Y. Shin, K. Lee, Y. Kim, J. Chang, W. Cho and K. Bae, *Int. J. Hydrogen Energy*, **37**, 16604 (2012).
19. C. L. Yaws, *Thermophysical properties of chemicals and hydrocarbons*, 1st Ed., William Andrew (2008).
20. B. E. Poling, J. M. Prausnitz and J. P. O'Connell, *The properties of gases and liquids*, 5th Ed. McGraw-Hill (2000).
21. D. R. Lide, *CRC handbook of chemistry and physics*, 87th Ed. CRC Press (2006).
22. D. W. Green and R. H. Perry, *Perry's chemical engineers' handbook*, 8th Ed. McGraw-Hill (2007).
23. P. M. Mathias, *Modeling the sulfur iodine cycle, Aspen building blocks and simulation models*, Report to General Atomics and Sandia National Laboratory (2002).
24. P. Wang, A. Anderko, R. D. Springer and R. D. Young, *J. Mol. Liq.*, **125**, 37 (2006).
25. M. C. Annesini, F. Gironi, M. Lanchi, L. Marrelli and M. Maschietti, *Proc. ICheaP-8*, Ischia, Italy, 24-27 June (2007).
26. M. K. Hadj-Kali, V. Gerbaud, J.-M. Borgard, O. Baudouin, P. Floquet, X. Joulia and P. Carles, *Int. J. Hydrogen Energy*, **34**, 1696 (2009).
27. J. E. Murphy and J. P. O'Conell, *Fluid Phase Equilibr.*, **288**, 99 (2010).
28. S. Kasahara, *Appendix A: Chemical, thermodynamic, and transport properties of pure compounds and solutions*, in X. L. Yan and R. Hino Ed., *Nuclear Hydrogen Production Handbook*, CRC Press, 801 (2011).
29. Wikipedia, en.wikipedia.org/wiki/Hydrogen_iodide (Accessed June of 2015).
30. Material Safety Data Sheet, www.msds.com (Accessed June of 2015).
31. P. Patnaik, *Handbook of inorganic chemicals*, McGraw-Hill (2003).
32. KDB (Korea Thermophysical Properties Data Bank), www.cheric.org/research/kdb/ (Accessed June of 2015).
33. NIST Chemistry Webbook, webbook.nist.gov (Accessed June of 2015).
34. W. F. Giauque and R. Wiebe, *J. Am. Chem. Soc.*, **51**, 1441 (1929).
35. S. Kubo, K. Yoshino, J. Takemoto, S. Kasahara, Y. Imai and K. Onuki, *Density of Bunsen reaction solution and viscosity of polyhydriodic acid*, JAEA-Technology, 2012-037 (2013). [In Japanese].
36. E. Nishikata, T. Ishii and T. Ohta, *J. Chem. Eng. Data*, **26**, 254 (1981).
37. T. M. Herrington, A. D. PethyBridge and M. G. Roffey, *J. Chem. Eng. Data*, **30**, 264 (1985).